# HETEROCLINIC CYCLES IN SYSTEMS WITH $\mathbf{D}_n$ SYMMETRY

Pietro-Luciano Buono[1], Martin Golubitsky[2]
and Antonio Palacios[2]
[1] Département de mathématiques et statistique
Université d'Ottawa ,Ottawa, Ont, Canada K1N 6N5
[2] Department of Mathematics, University of Houston
Houston, TX 77204-3476, USA

**Abstract**

In this paper we investigate numerically the existence of heteroclinic cycles connecting periodic solutions and equilibria in systems of differential equations with dihedral $\mathbf{D}_n$ symmetry. We study these cycles near steady-state/Hopf and Hopf/Hopf mode interaction points. The existence of these cycles depends on normal form symmetries and their construction is based on the lattice of isotropy subgroups. A variety of interesting forms of intermittency are found and illustrated.

## 1 INTRODUCTION

In the simplest cases heteroclinic cycles consist of trajectories in a differential equation that form a ring by connecting sequences of equilibria. Field [4] and Guckenheimer and Holmes [6] observed that such cycles can be structurally stable in systems with symmetry. When a heteroclinic cycle is also asymptotically stable, it serves as a model for a certain kind of intermittency, since nearby trajectories move quickly between the equilibria and stay for a relatively long time near each equilibria. Aubry *et al.* [2] use asymptotically stable heteroclinic cycles to study boundary layer turbulence in channel flow.

Armbruster, Guckenheimer, and Holmes [1] show that heteroclinic cycles appear in the unfolding of steady-state/steady-state mode interactions with $\mathbf{O}(2)$ symmetry. Melbourne, Chossat, and Golubitsky [8] provide a general approach for finding heteroclinic connections in equivariant systems of ODEs and use this approach to find heteroclinic cycles specifically for $\mathbf{O}(2)$ symmetric problems. The authors demonstrate that by restricting the vector field to flow invariant subspaces, it is possible to find heteroclinic cycles. The basic idea is as follows. Suppose that $\Gamma$ is the symmetry group for a system of differential equations and that $\Sigma \subset \Gamma$ is a subgroup. It is well known that the fixed-point subspace

$$\mathrm{Fix}(\Sigma) = \{x \in \mathbf{R}^n : \sigma x = x \quad \forall \sigma \in \Sigma\}$$

is a flow invariant subspace [5]. The idea in [8] is to find a sequence of maximal isotropy subgroups $\Sigma_j$ and corresponding submaximal isotropy subgroups $T_j$ such as is shown schematically in Figure 1. Such configurations of isotropy subgroups have the possibility of leading to heteroclinic cycles if differential equations can be found connecting equilibria in $\mathrm{Fix}(\Sigma_j)$ to $\mathrm{Fix}(\Sigma_{j+1})$ via a saddle sink connection in $\mathrm{Fix}(T_j)$.

$$\begin{tikzcd}
\Sigma_1 & & \Sigma_2 & & \cdots & & \Sigma_{k-1} & & \Sigma_1 \\
& \mathbf{T}_1 \arrow[ul] \arrow[ur] & & \mathbf{T}_2 \arrow[ul] \arrow[ur] & & \mathbf{T}_{k-1} \arrow[ul] \arrow[ur] & & \mathbf{T}_k \arrow[ul] \arrow[ur] &
\end{tikzcd}$$

Figure 1: Pattern inside the isotropy lattice that permits, in some cases, the existence of heteroclinic cycles.

Melbourne *et al.* [8] also generalize the notion of heteroclinic cycles to include time periodic solutions as well as equilibria. They do this by augmenting the symmetry group of the differential equations with $\mathbf{S}^1$ — the symmetry group of Poincaré-Birkhoff normal form near points of Hopf bifurcation — and using phase-amplitude equations in the analysis. Indeed, as shown by Melbourne [7], normal form symmetry is sufficient to produce stable cycling behavior in systems without spatial symmetry.

It is well-known that Hopf bifurcation from an invariant equilibrium in systems with $\mathbf{O}(2)$ symmetry leads to two types of periodic solutions: *standing waves* (solutions invariant under a single reflection for all time) and *rotating waves* (solutions whose time evolution is the same as spatial rotation) [5]. Melbourne *et al.* [8] prove the existence of structurally stable, asymptotically stable heteroclinic cycles involving time periodic solutions in steady-state/Hopf and Hopf/Hopf mode interactions in systems with $\mathbf{O}(2)$ symmetry. More precisely, consider an $\mathbf{O}(2)$-equivariant differential equation of the form

$$\frac{dx}{dt} = F(x, \lambda, \mu), \tag{1.1}$$

where $x \in \mathbf{R}^N$, $\lambda \in \mathbf{R}$ is a distinguished bifurcation parameter and $\mu \in \mathbf{R}$ is an auxiliary parameter. Analysis of the normal form equations at such mode interactions leads to a variety of heteroclinic cycles.

For example, Figure 2 shows a cycle connecting a steady-state with a standing wave. The steady-state/Hopf mode interaction has a six-dimensional center manifold, since each critical eigenvalue is doubled by symmetry. Figure 2 shows the time series from three coordinates: $x_0$ is a coordinate in the steady-state mode and $x_1, x_2$ are coordinates in the Hopf mode.

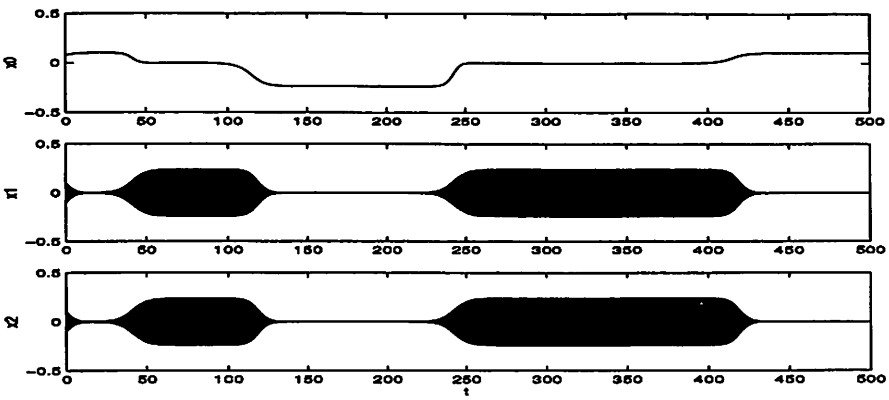


Figure 2: Cycle connecting a steady-state with a standing wave in a system with $\mathbf{O}(2) \times \mathbf{S}^1$ symmetry with $\mathbf{S}^1$ due to normal form.

Figure 3 shows a cycle between two standing waves and two rotating waves stemming from a Hopf/Hopf mode interaction. Again the critical eigenvalues are doubled by $\mathbf{O}(2)$ symmetry so that the center manifold is eight-dimensional. The time series for four of these coordinates are shown in Figure 3 with two coordinates from each mode. In these coordinates a standing wave in one mode is an oscillation with both coordinates oscillating equally (with a phase shift) while a rotating wave is an oscillation with one coordinate active and the other coordinate quiescent. Using this description we can see that the time series in Figure 3 begins near a standing wave in the first mode, then transitions to a standing wave in the second mode, then to a rotating wave in the second mode, followed by a rotating wave in the first mode. The cycle then repeats forever. In this way the spatial and temporal structure of the numerical solutions reflect the symmetries of the solutions visited by the trajectory.

In this paper, we explore numerically the existence of heteroclinic cycles when $\mathbf{O}(2)$ symmetry is replaced by $\mathbf{D}_n$ symmetry. Here we show that cycles corresponding to those in Figures 2 and 3 for systems with $\mathbf{O}(2)$ symmetry also occur in systems with $\mathbf{D}_n$ symmetry. These cycles are richer in that they connect equilibria and time periodic solutions with more types of symmetry. Moreover, these cycles can appear in rings of coupled cells — though to prove that statement requires performing the details of center manifold reductions — where the manifestation of the spatial-temporal symmetries is quite interesting. This topic will be discussed in detail and with proofs in [3]. In Section 2 we discuss the group actions of $\mathbf{D}_n$ and normal form at points of $\mathbf{D}_n$ mode interaction. In Section 3 we illustrate our results on $\mathbf{D}_n$ steady-

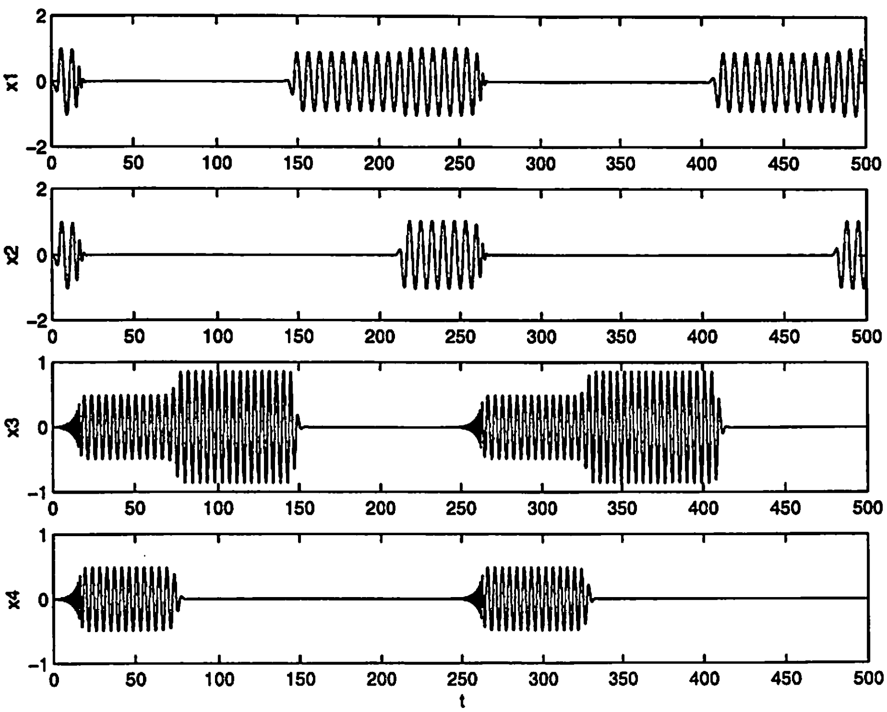


Figure 3: Cycle connecting rotating waves with standing waves in a system with $\mathbf{O}(2) \times \mathbf{T}^2$ symmetry with $\mathbf{T}^2$ due to normal form.

state/Hopf mode interactions and in Section 4 we illustrate our results on $\mathbf{D}_n$ Hopf/Hopf mode interactions.

# 2 $\mathbf{D}_n$ MODE INTERACTIONS

Consider a system of ODEs such as (1.1) but assume now that $F$ is $\mathbf{D}_n$-equivariant, and that $x = 0$ is a $\mathbf{D}_n$-symmetric *trivial* solution, that is,

$$F(0, \lambda, \mu) = 0.$$

Assume also that the Jacobian $(d_x F)_{0,0,0}$ has multiple eigenvalues lying on the imaginary axis, each of multiplicity two due to symmetry. We consider two cases: (1) 0, $\pm\omega i$ and (2) $\pm\omega_1 i$, $\pm\omega_2 i$, where $\omega_1$ and $\omega_2$ are incommensurate. The former case is a steady-state/Hopf mode interaction and the later a nonresonant Hopf/Hopf mode interaction. Moreover, in this paper, we assume that $\mathbf{D}_n$ acts by its standard action on each of the critical eigenspaces.

After performing a center manifold reduction on (1.1), we arrive at the reduced system of ODEs

$$\frac{dz}{dt} = g(z, \lambda, \mu), \tag{2.1}$$

where $g(0, \lambda, \mu) = 0$. In the steady-state/Hopf case $z \in \mathbf{C}^3$, and in the Hopf/Hopf case $z \in \mathbf{C}^4$. The eigenvalues of $(d_z g)_{0,0,0}$ are those of $(d_x F)_{0,0,0}$ on the imaginary axis. By an appropriate change of coordinates we can assume that (2.1) is in Poincaré-Birkhoff normal form up to any finite order. This introduces an extra symmetry, so that in the steady-state/Hopf case $g$ is $\mathbf{D}_n \times \mathbf{S}^1$-equivariant. We can then choose coordinates $z = (z_0, z_1, z_2)$ such that the $\mathbf{D}_n \times \mathbf{S}^1$-action on $\mathbf{C}^3$ takes the following form. Let $\gamma = 2\pi/n \in \mathbf{Z}_n$ and $\theta \in \mathbf{S}^1$, and let $\kappa$ be a fixed element in $\mathbf{D}_n \sim \mathbf{Z}_n$. Then

$$\begin{aligned}
\gamma(z_0, z_1, z_2) &= (e^{\gamma i} z_0, e^{\gamma i} z_1, e^{-\gamma i} z_2) \\
\kappa(z_0, z_1, z_2) &= (\bar{z}_0, z_2, z_1) \\
\theta(z_0, z_1, z_2) &= (z_0, e^{\theta i} z_1, e^{\theta i} z_2).
\end{aligned}$$

In the Hopf/Hopf case, $g$ is $\mathbf{D}_n \times \mathbf{T}^2$-equivariant when in normal form. In a similar way, we choose coordinates $z = (z_1, z_2, z_3, z_4)$ such that the $\mathbf{D}_n \times \mathbf{T}^2$-action on $\mathbf{C}^4$ takes the following form. Let $\gamma$ and $\kappa$ be in $\mathbf{D}_n$, as above, and let $(\theta_1, \theta_2) \in \mathbf{T}^2$. Then

$$\begin{aligned}
\gamma(z_1, z_2, z_3, z_4) &= (e^{i\gamma} z_1, e^{-i\gamma} z_2, e^{i\gamma} z_3, e^{-i\gamma} z_4) \\
\kappa(z_1, z_2, z_3, z_4) &= (z_2, z_1, z_4, z_3) \\
(\theta_1, \theta_2)(z_1, z_2, z_3, z_4) &= (e^{i\theta_1} z_1, e^{i\theta_1} z_2, e^{i\theta_2} z_3, e^{i\theta_2} z_4).
\end{aligned}$$

# 3 STEADY-STATE/HOPF MODES

Let $\delta = |z_2|^2 - |z_1|^2$. The $\mathbf{D}_6 \times \mathbf{S}^1$-invariant functions are functions of

$$\begin{array}{lll}
\rho = |z_o|^2 & N = |z_1|^2 + |z_2|^2 & \Delta = \delta^2 \\
A = z_0^2 \bar{z}_1 z_2 + \bar{z}_0^2 z_1 \bar{z}_2 & B = z_0^6 + \bar{z}_0^6 & C = (z_1\bar{z}_2)^3 + (\bar{z}_1 z_2)^3 \\
D = z_0^2 (z_1 \bar{z}_2)^2 + \bar{z}_0^2 (\bar{z}_1 z_2)^2 & E = z_0^4 z_1 \bar{z}_2 + \bar{z}_0^4 \bar{z}_1 z_2. &
\end{array}$$

The $\mathbf{D}_6 \times \mathbf{S}^1$-equivariant vector field has the form $g(z, \lambda, \mu) = (C(z), P(z)) \in \mathbf{C} \times \mathbf{C}^2$ where

$$C(z) = C^1 z_0 + C^3 \bar{z}_0 z_1 \bar{z}_2 + C^5 \bar{z}_0^5 + C^7 \bar{z}_0 (\bar{z}_1 z_2)^2 + C^9 \bar{z}_0^3 \bar{z}_1 z_2 + C^{11} z_0 (z_1 \bar{z}_2)^3$$

and

$$\begin{aligned}
P(z) = {} & P^1 \begin{bmatrix} z_1 \\ z_2 \end{bmatrix} + P^2 \delta \begin{bmatrix} z_1 \\ -z_2 \end{bmatrix} + P^3 \begin{bmatrix} z_0^2 z_2 \\ \bar{z}_0^2 z_1 \end{bmatrix} + P^4 \delta \begin{bmatrix} z_0^2 z_2 \\ -\bar{z}_0^2 z_1 \end{bmatrix} \\
& + P^5 \begin{bmatrix} |z_2|^2 z_1 \\ |z_1|^2 z_2 \end{bmatrix} + P^6 \delta \begin{bmatrix} |z_2|^2 z_1 \\ -|z_1|^2 z_2 \end{bmatrix} + P^7 \begin{bmatrix} \bar{z}_0^4 z_2 \\ z_0^4 z_1 \end{bmatrix} \\
& + P^8 \delta \begin{bmatrix} \bar{z}_0^4 z_2 \\ -z_0^4 z_1 \end{bmatrix} + P^9 \begin{bmatrix} \bar{z}_0^2 \bar{z}_1 z_2^2 \\ z_0^2 z_1^2 \bar{z}_2 \end{bmatrix} + P^{10} \delta \begin{bmatrix} \bar{z}_0^2 \bar{z}_1 z_2^2 \\ -z_0^2 z_1^2 \bar{z}_2 \end{bmatrix} \\
& + P^{11} \begin{bmatrix} (\bar{z}_1 z_2)^2 z_2 \\ (z_1 \bar{z}_2)^2 z_1 \end{bmatrix} + P^{12} \delta \begin{bmatrix} (\bar{z}_1 z_2)^2 z_2 \\ -(z_1 \bar{z}_2)^2 z_1 \end{bmatrix}
\end{aligned} \tag{3.1}$$

where $c^j$ are real-valued $\mathbf{D}_6 \times \mathbf{S}^1$-invariant functions and $P^j$ are complex-valued $\mathbf{D}_6 \times \mathbf{S}^1$-invariant functions depending on two parameters $\lambda$ and $\mu$, and $C^j = c^j + i\delta c^{j+1}$. Additionally, the eigenvalue structure of $g$ leads to $c^1(0) = 0$ and $P^1(0) = \omega i$. See [3].

We next search for heteroclinic cycles as solutions of $g$ by considering the lattice of isotropy subgroups shown in Figure 4. Following [8] the lattice

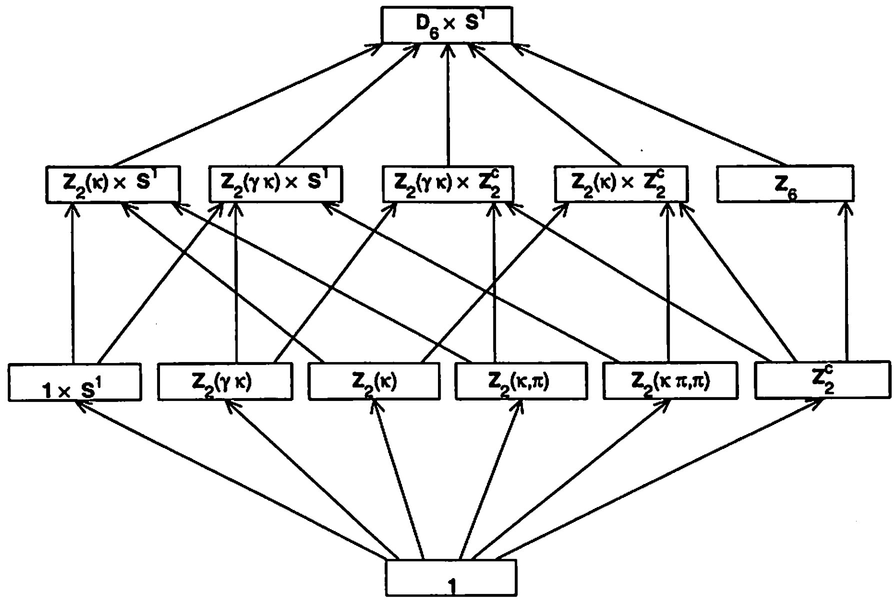


Figure 4: Isotropy lattice of $\mathbf{D}_6 \times \mathbf{S}^1$ acting on $\mathbf{C}^3$

suggests the possible existence of a heteroclinic cycle. This cycle contains a trajectory that connects a steady state $e_1$ (with $\mathbf{Z}_2(\kappa) \times \mathbf{S}^1$ symmetry) with a standing wave $SW_1$ (with $\mathbf{Z}_2(\kappa) \times \mathbf{Z}_2^c$ symmetry) through the invariant subspace $\mathbf{Z}_2(\kappa)$. The standing wave $SW_1$ is then connected with another steady state $e_2$ (with $\mathbf{Z}_2(\gamma\kappa) \times \mathbf{S}^1$ symmetry) through the invariant subspace $\mathbf{Z}_2(\kappa\pi, \pi)$. The trajectory then connects the equilibrium $e_2$ to a second standing wave $SW_2$ (with $\mathbf{Z}_2(\gamma\kappa) \times \mathbf{Z}_2^c$ symmetry) through the invariant subspace $\mathbf{Z}_2(\gamma\kappa)$. The cycle is completed by a trajectory connecting $SW_2$ to the first steady state $e_1$ through $\mathbf{Z}_2(\kappa, \pi)$.

Using the general $\mathbf{D}_6 \times \mathbf{S}^1$-equivariant map (3.1), we numerically integrate the system (2.1) with the following coefficients:

$$\begin{array}{llll} c^1 = \lambda - 1.5\rho - 4N & c^2 = 1.3 & c^3 = -9 & c^5 = 0.5 \\ p^1 = 1.2\lambda - 3\rho - N & p^{11} = 4 & p^2 = 4 & p^3 = 4 \\ q^1 = 0.8\lambda + 7 & q^{11} = 8 & & \end{array}$$

and all other coefficients set to zero. The results are shown in Figure 5. The difference between the two standing waves $SW1$ and $SW2$ can be visualized by enlarging the components of $z_1$ or $z_2$. For instance, Figure 6 depicts an enlarged region of $\mathrm{Re}(z_1)$ and shows two standing waves with different amplitudes.

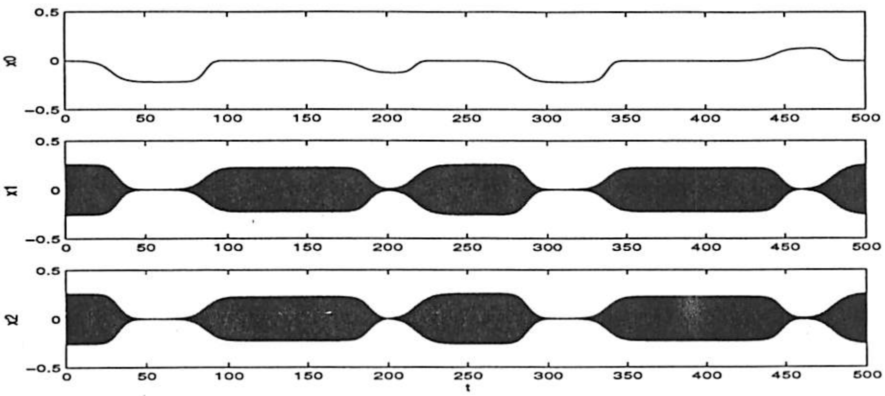


Figure 5: Heteroclinic cycle connecting steady states $e_1$ and $e_2$ with standing waves $SW_1$ and $SW_2$ in a system with $\mathbf{D}_6 \times \mathbf{S}^1$ symmetry.

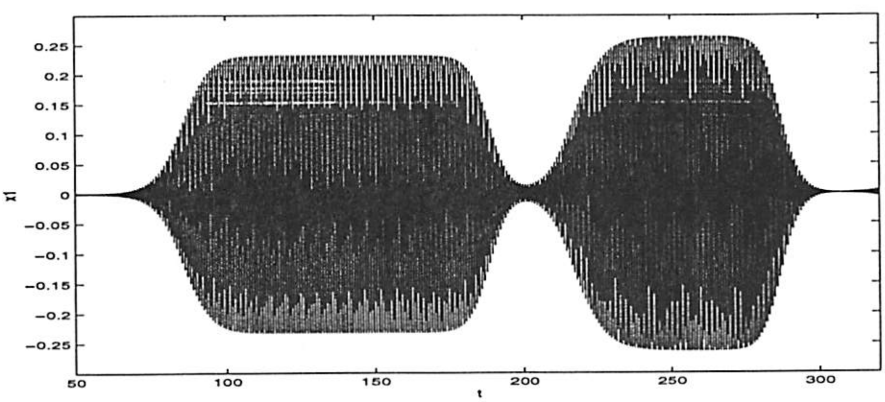


Figure 6: Enlargement of time series $x_1$ from Figure 5 showing standing waves with different amplitudes.

The isotropy lattice for the case $n = 5$ is shown in Figure 7. Observe that, in this case, the lattice appears to lack the structure described in Figure 1. This does not prevent the existence of intermittent behavior in (1.1).

In order to understand what happens to the cycle when the $\mathbf{O}(2)$ symmetry is broken, we approach the case $n = 5$ as a symmetry-breaking perturbation from $\mathbf{O}(2)$ to $\mathbf{D}_5$ symmetry. The general $\mathbf{D}_5 \times \mathbf{S}^1$-equivariant map

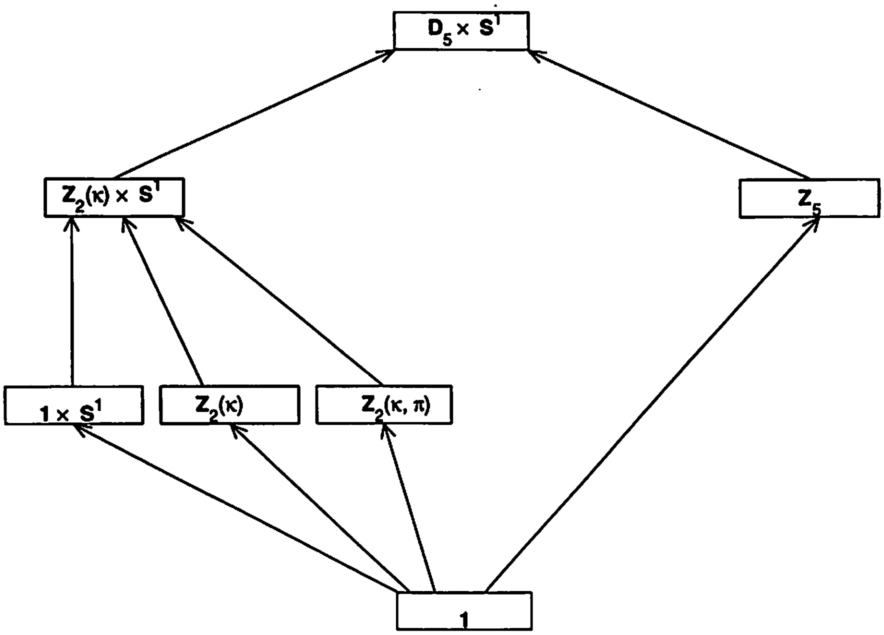


Figure 7: Isotropy lattice of $\mathbf{D}_5 \times \mathbf{S}^1$ acting on $\mathbf{C}^3$

is $g(z,\lambda,\mu) = (C(z), P(z)) \in \mathbf{C} \times \mathbf{C}^2$ where

$$C(z) = C^1 z_0 + C^3 \bar{z}_0 z_1 \bar{z}_2 + C^5 \bar{z}_0^4 + C^7 (\bar{z}_1 z_2)^2 + C^9 \bar{z}_0^2 \bar{z}_1 z_2 + C^{11} (z_1 \bar{z}_2)^3$$

and

$$\begin{aligned}
P(z) = {} & P^1 \begin{bmatrix} z_1 \\ z_2 \end{bmatrix} + P^2 \delta \begin{bmatrix} z_1 \\ -z_2 \end{bmatrix} + P^3 \begin{bmatrix} z_0^2 z_2 \\ \bar{z}_0^2 z_1 \end{bmatrix} + P^4 \delta \begin{bmatrix} z_0^2 z_2 \\ -\bar{z}_0^2 z_1 \end{bmatrix} \\
& + P^5 \begin{bmatrix} |z_2|^2 z_1 \\ |z_1|^2 z_2 \end{bmatrix} + P^6 \delta \begin{bmatrix} |z_2|^2 z_1 \\ -|z_1|^2 z_2 \end{bmatrix} + P^7 \begin{bmatrix} \bar{z}_0^3 z_2 \\ z_0^3 z_1 \end{bmatrix} + \\
& P^8 \delta \begin{bmatrix} \bar{z}_0^3 z_2 \\ -z_0^3 z_1 \end{bmatrix} + P^9 \begin{bmatrix} \bar{z}_0 \bar{z}_1 z_2^2 \\ z_0 z_1^2 \bar{z}_2 \end{bmatrix} + P^{10} \delta \begin{bmatrix} \bar{z}_0 \bar{z}_1 z_2^2 \\ -z_0 z_1^2 \bar{z}_2 \end{bmatrix} + \\
& P^{11} \begin{bmatrix} z_0 (\bar{z}_1 z_2)^2 z_2 \\ \bar{z}_0 (z_1 \bar{z}_2)^2 z_1 \end{bmatrix} + P^{12} \delta \begin{bmatrix} z_0 (\bar{z}_1 z_2)^2 z_2 \\ -\bar{z}_0 (z_1 \bar{z}_2)^2 z_1 \end{bmatrix} + \\
& P^{13} \begin{bmatrix} (\bar{z}_1 z_2)^4 z_2 \\ (z_1 \bar{z}_2)^4 z_1 \end{bmatrix} + P^{14} \delta \begin{bmatrix} (\bar{z}_1 z_2)^4 z_2 \\ -(z_1 \bar{z}_2)^4 z_1 \end{bmatrix}
\end{aligned} \tag{3.2}$$

We integrate numerically the general $\mathbf{D}_5 \times \mathbf{S}^1$-equivariant map (3.2) with the following coefficients:

$$\begin{array}{lllll}
c^1 = \lambda - 1.5\rho - 4N & c^2 = 1.3 & c^3 = -9 & c^5 = 0.5 & q^1 = 0.8\lambda + 7 \\
p^1 = 1.2\lambda - 3\rho - N & p^3 = 4 & p^{13} = 4 & q^{11} = 8 &
\end{array}$$

and all other coefficients set to zero. The results are shown in Figure 8.

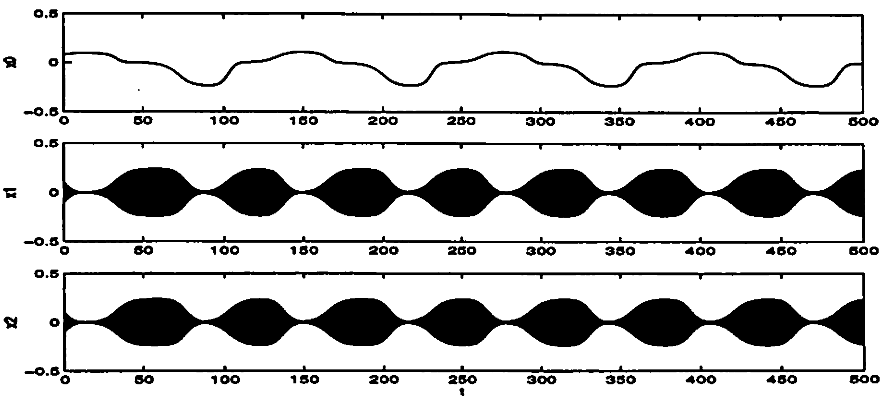


Figure 8: Trajectory visiting intermittently a steady-state and a standing wave after the heteroclinic cycle of Figure 2 is broken by a $\mathbf{D}_5 \times \mathbf{S}^1$-equivariant perturbation.

# 4 HOPF/HOPF MODES

Let $\delta_0 = 1$, $\delta_1 = |z_2|^2 - |z_1|^2$, and $\delta_2 = |z_4|^2 - |z_3|^2$; and let $v_{12} = z_1\overline{z_2}$ and $v_{34} = z_3\overline{z_4}$. The general $\mathbf{D}_n \times \mathbf{T}^2$-invariant function is a function of

$$\begin{array}{llll} N_1 = |z_1|^2 + |z_2|^2 & \Delta_1 = \delta_1^2 & \Delta_{12} = \delta_1\delta_2 & \\ N_2 = |z_3|^2 + |z_4|^2 & \Delta_2 = \delta_2^2 & v_i = \mathrm{Re}(v_{12}^{m-i} v_{34}^{i}) & 0 \le i \le m, \end{array}$$

where

$$m = \begin{cases} n & \text{if } n \text{ is odd} \\ n/2 & \text{if } n \text{ is even.} \end{cases}$$

The general $\mathbf{D}_n \times \mathbf{T}^2$-equivariant mapping is given by $g(z,\lambda,\mu) =$

$$A^1 \begin{bmatrix} z_1 \\ z_2 \\ z_3 \\ z_4 \end{bmatrix} + (A^3\delta_1 + A^5\delta_2) \begin{bmatrix} z_1 \\ -z_2 \\ z_3 \\ -z_4 \end{bmatrix} + (A^7 + A^9\delta_1 + A^{11}\delta_2) \begin{bmatrix} z_2 v_{34} \\ z_1\overline{v_{34}} \\ z_4 v_{12} \\ z_3\overline{v_{12}} \end{bmatrix}$$

$$+A^{13} \begin{bmatrix} z_1 v_{12}\overline{v_{34}} \\ z_2\overline{v_{12}}v_{34} \\ z_3\overline{v_{12}}v_{34} \\ z_4 v_{12}\overline{v_{34}} \end{bmatrix} + \sum_{i=0}^{m-1}\sum_{j=0}^{2} Q_{j+1}^{2i+1}\delta j \begin{bmatrix} \overline{v_{12}}^{m-1-i}\overline{v_{34}}^{i} z_2 \\ v_{12}^{m-1-i} v_{34}^{i} z_1 \\ \overline{v_{34}}^{m-1-i}\overline{v_{12}}^{i} z_4 \\ v_{34}^{m-1-i} v_{12}^{i} z_3 \end{bmatrix} \tag{4.1}$$

where $A^j$ and $Q_l^j$ are complex-valued $\mathbf{D}_n \times \mathbf{T}^2$-invariant functions of two parameters $\lambda$ and $\mu$, and

$$A^j = \begin{bmatrix} a^j + ia^{j+1} \\ a^j + ia^{j+1} \\ b^j + ib^{j+1} \\ b^j + ib^{j+1} \end{bmatrix}, \quad Q_l^j = \begin{bmatrix} q_l^j + iq_l^{j+1} \\ q_l^j + iq_l^{j+1} \\ r_l^j + ir_l^{j+1} \\ r_l^j + ir_l^{j+1} \end{bmatrix}.$$

Note that the eigenvalue structure of $g$ leads to $a^1(0) = b^1(0) = 0$ and $a^2(0) = \omega_1 i$ and $b^2(0) = \omega_2 i$ where $\omega_1$ and $\omega_2$ are incommensurate. See [3].

We look for heteroclinic cycles in the vector field $g$ by inspection of the isotropy lattice. Let $n$ be odd or $n \equiv 2 \pmod 4$ (see [3] for the case $n \equiv 0 \pmod 4$) and define

$$\mathbf{Z}_2^{cn} = \begin{cases} <(\pi,\pi,\pi)> & \text{if } n \text{ is even} \\ 1 & \text{if } n \text{ is odd.} \end{cases}$$

and let

$$\mathbf{Z}_n(k,l,m) \equiv \{(k\gamma, l\gamma, m\gamma) \in \mathbf{Z}_n^3 : k,l,m \in \mathbf{Z}\},$$

where $\gamma$ is the generator of $\mathbf{Z}_n$, and

$$\mathbf{S}^1(1,0) \equiv \{(\theta,0) \in \mathbf{T}^2 : \theta \in \mathbf{S}^1\} \text{ and } \mathbf{S}^1(0,1) \equiv \{(0,\theta) \in \mathbf{T}^2 : \theta \in \mathbf{S}^1\}.$$

Part of the isotropy lattice of the action of $\mathbf{D}_n \times \mathbf{T}^2$ on $\mathbf{C}^4$ is given in Figure 9 and the isotropy subgroups are listed in Table 1.

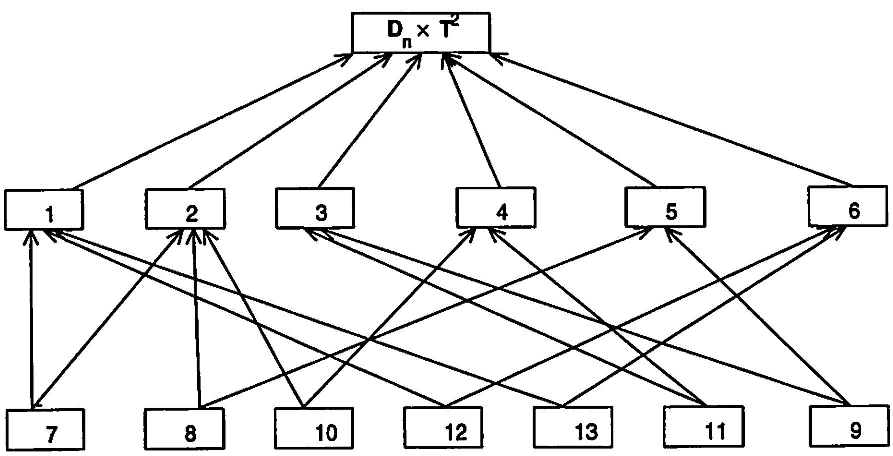


Figure 9: Part of the lattice of isotropy subgroups of $\mathbf{D}_n \times \mathbf{T}^2$

The isotropy lattice suggests the possible presence of three heteroclinic cycles analogous to the ones found in the $\mathbf{O}(2)$ symmetric system [8]. However, in $\mathbf{D}_n$ Hopf bifurcation, there are two types of standing waves bifurcating simultaneously, one with isotropy $\mathbf{Z}_2(\kappa)$ and one with isotropy $\mathbf{Z}_2(\kappa, \pi)$,

|  | Isotropy Subgroup |  | Isotropy Subgroup |
|---|---|---|---|
| (1) | $\mathbf{Z}_n(1,-1,0) \times \mathbf{S}^1(0,1)$ | (8) | $\mathbf{Z}_2(\kappa) \times \mathbf{Z}_2^{cn}$ |
| (2) | $\mathbf{Z}_2(\kappa) \times \mathbf{Z}_2^{cn} \times \mathbf{S}^1(0,1)$ | (9) | $\mathbf{Z}_2(\kappa,\pi,0) \times \mathbf{Z}_2^{cn}$ |
| (3) | $\mathbf{Z}_2(\kappa,\pi,0) \times \mathbf{Z}_2^{cn} \times \mathbf{S}^1(0,1)$ | (10) | $\mathbf{Z}_2(\kappa,0,\pi) \times \mathbf{Z}_2^{cn}$ |
| (4) | $\mathbf{Z}_2(\kappa,0,\pi) \times \mathbf{Z}_2^{cn} \times \mathbf{S}^1(1,0)$ | (11) | $\mathbf{Z}_2(\kappa,\pi,\pi) \times \mathbf{Z}_2^{cn}$ |
| (5) | $\mathbf{Z}_2(\kappa) \times \mathbf{Z}_2^{cn} \times \mathbf{S}^1(1,0)$ | (12) | $\mathbf{Z}_n(1,-1,1)$ |
| (6) | $\mathbf{Z}_n(1,0,1) \times \mathbf{S}^1(1,0)$ | (13) | $\mathbf{Z}_n(1,1,1)$ |
| (7) | $\mathbf{S}^1(0,1)$ |  |  |

Table 1: Isotropy subgroups

see [5]. Note that the standing waves with isotropy (2) and (5) are of type $\mathbf{Z}_2(\kappa)$ and that the standing waves with isotropy (3) and (4) are of type $\mathbf{Z}_2(\kappa,\pi)$. The three possible cycles are the following.

The first is a cycle between rotating waves. A trajectory connects rotating wave (1) to rotating wave (6) through the fixed-point subspace of (12) and the cycle is completed by a trajectory connecting back to (1) through the fixed-point subspace of (13).

The second cycle connects the standing wave with isotropy subgroup (2) with the standing wave with isotropy (4) through the fixed-point subspace of (10), the standing wave with isotropy (4) with the standing wave (3) through the fixed-point subspace of (11), then (3) is connected to the standing wave (5) through the fixed-point subspace of (9) and finally (5) is connected to (2) through the fixed-point subspace of (8). The proof of existence of the first two cycles is found in [3].

Finally, according to the lattice, a cycle between rotating waves and standing waves can also exist in principle. However, the fixed-point subspace of (7) where the connection between rotating wave (1) and standing wave (2) should lie does not decouple completely in phase-amplitude coordinates, therefore the existence of a connection is unlikely.

We find the cycle joining standing waves by integrating numerically the general $\mathbf{D}_5 \times \mathbf{T}^2$-equivariant map (4.1). We set $m = 5$, and let

$$\begin{array}{llll} a^1 = \lambda - N_1 - 2.5N_2 & a^2 = 1 & a^3 = 2.5 & a^4 = 0.5 \\ & a^7 = 2 & q_1^1 = 0.3 & q_1^2 = -0.2 \\ b^1 = \lambda - 2N_1 - 2N_2 & b^2 = 1.41 & b^5 = 1.5 & b^6 = -0.25 \\ & b^7 = -3 & r_1^1 = -0.45 & r_1^2 = 0.15, \end{array}$$

and all other coefficients are set to zero. The simulation is shown in Figure 10.

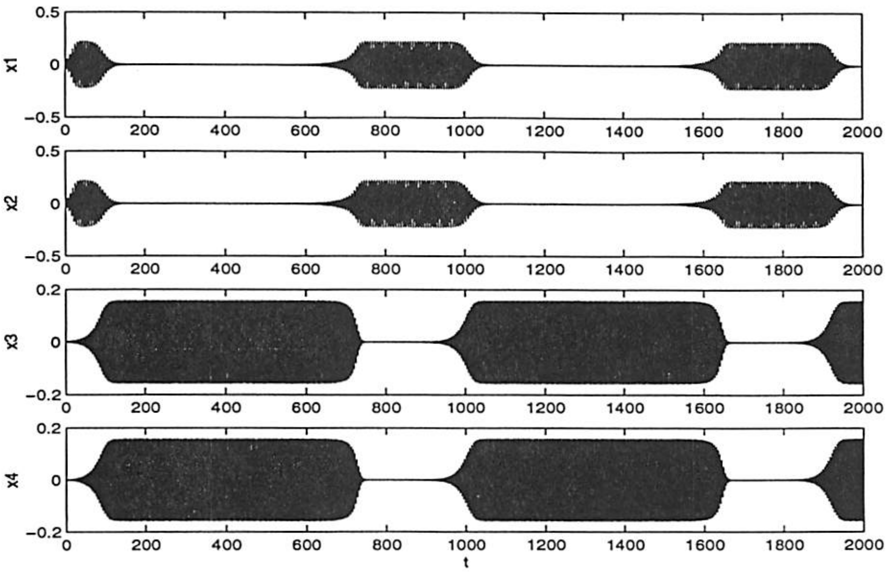


Figure 10: Cycle joining standing waves in $\mathbf{D}_5 \times \mathbf{T}^2$-equivariant system.

Even though a cycle between rotating waves and standing waves is unlikely in $\mathbf{D}_n \times \mathbf{T}^2$-equivariant system, we can still find intermittent behavior between rotating waves and standing waves. Figure 11 shows a trajectory close to the attractor that persists when a $\mathbf{D}_5 \times \mathbf{T}^2$ perturbation is added to an $\mathbf{O}(2) \times \mathbf{T}^2$ system with a heteroclinic cycle that joins rotating waves with standing waves as in Figure 3. The simulation in Figure 11 is done by integrating equation (4.1) with $m = 5$ and

$$\begin{array}{llll}
a^1 = \lambda + 0.9i - 0.375N_1 - 3.55N_2 & a^2 = 0.9 & a^3 = 0.625 & a^5 = -3.45 \\
a^7 = 0.125 & a^8 = 7 & q_1^1 = 0.003 & q_1^2 = 0.002 \\
b^1 = \lambda - 1.75N_1 - 1.667N_2 & b^2 = 1.4 & b^3 = 0.25 & b^5 = -0.583 \\
b^7 = 3 & b^8 = 6 & r_1^1 = 0.008 & r_1^2 = 0.004.
\end{array}$$

Figure 12 shows the $x_3$ and $x_4$ coordinates of the trajectory of Figure 11 as it approaches standing wave (5). Figure 13 shows the same coordinates of Figure 11 as the trajectory gets close to standing wave (4). Note that the time series in Figure 12 near the periodic solution are in phase while the time series in Figure 13 near the periodic solution are one half-period out of phase.

## ACKNOWLEDGMENTS

We wish to thank Ian Melbourne for a number of helpful conversations. This research was supported in part by NSF Grant DMS-9704980 and the Texas

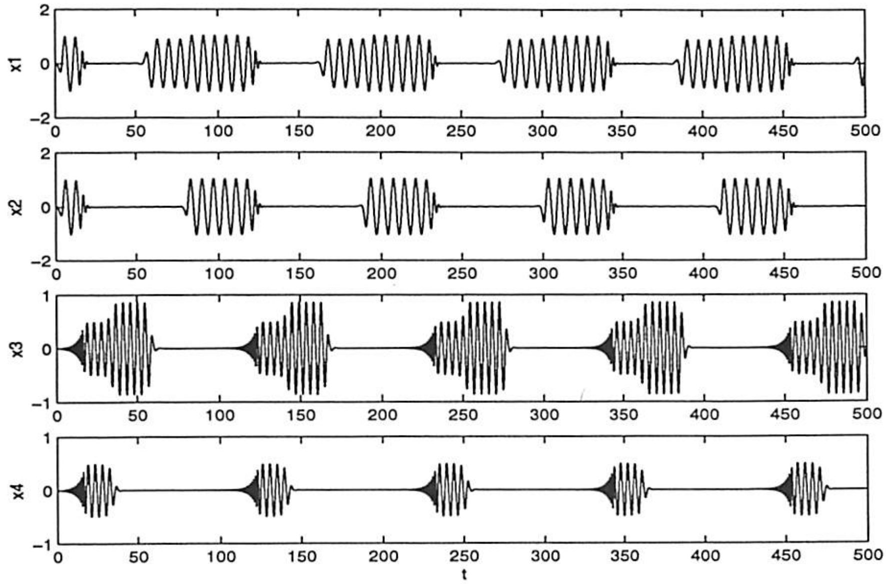


Figure 11: Trajectory visiting intermittently rotating waves and standing waves of type $\mathbf{Z}_2(\kappa)$ and $\mathbf{Z}_2(\kappa, \pi)$ after the cycle of Figure 3 is broken by a $\mathbf{D}_5 \times \mathbf{T}^2$-equivariant perturbation.

Advanced Research Program (003652037).

# References

[1] D. Armbruster, J. Guckenheimer, and P. Holmes. Heteroclinic cycles and modulated travelling waves in systems with $\mathbf{O}(2)$ symmetry, *Physica D* **29** (1988) 257–282.

[2] N. Aubry, P. Holmes, J. Lumley, and E. Stone. The dynamics of coherent structures in a wall region of a turbulent boundary layer, *J. Fluid Mech.* **192** (1988) 115–173.

[3] P-L. Buono, M. Golubitsky, and A. Palacios. Heteroclinic cycles in rings of coupled cells. In preparation.

[4] M. J. Field. Equivariant dynamical systems, *Trans. Amer. Math. Soc.*, **259**(1) (1980) 185–205.

[5] M. Golubitsky, I.N. Stewart, and D.G. Schaeffer. *Singularities and Groups in Bifurcation Theory: Vol. II.* Applied Mathematical Sciences **69**, Springer-Verlag, New York, 1988.

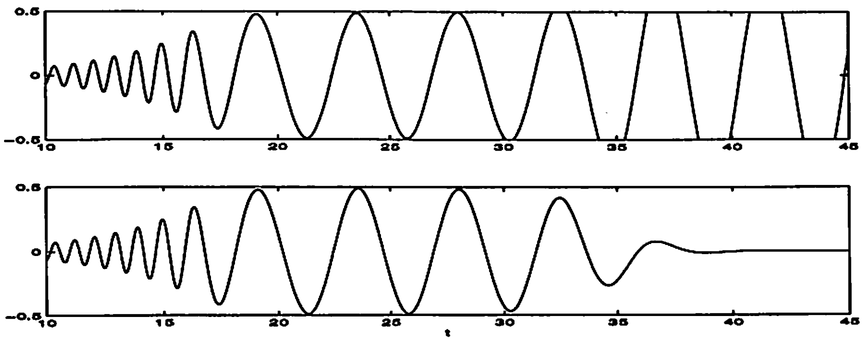

Figure 12: Enlargement of Figure 11 close to standing wave (5).

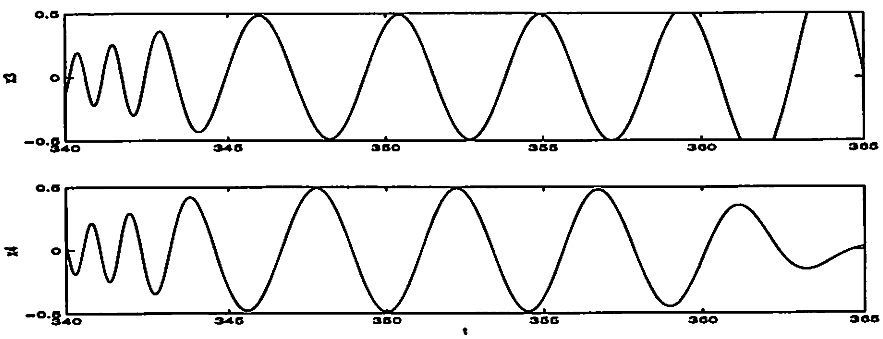

Figure 13: Enlargement of Figure 11 close to standing wave (4)


[6] J. Guckenheimer and P. Holmes. Structurally stable heteroclinic cycles, *Math. Proc. Camb. Phil. Soc.* **103** (1988) 189–192.

[7] I. Melbourne. Intermittency as a codimension three phenomenon, *Dyn. Diff. Eqn.* 1 (1989) 347-367.

[8] I. Melbourne, P. Chossat, and M. Golubitsky. Heteroclinic cycles involving periodic solutions in mode interactions with **O**(2) symmetry, *Proc. Roy. Soc. Edinburgh* **113A** (1989) 315.